Acta Cryst. (1987). A43, 711-718

Scan-Truncation Corrections in Single-Crystal Diffractometry: an Empirical Method*

BY RICCARDO DESTRO† AND RICHARD E. MARSH

Arthur Amos Noyes Laboratory of Chemical Physics, California Institute of Technology, Pasadena, California 91125, *USA*

(*Received* 17 *September* 1986; *accepted* 8 *May* 1987)

Abstract

A satisfactory model for experimental θ-2θ scan profiles of single-crystal diffraction intensities can be obtained by convoluting the spectral dispersion with the intrinsic profile and then with a third angle-dependent function which we call an 'aberration function'. The first of these functions is calculated on the basis of theoretical components, while the other two are obtained from experimental measurements. The process includes accurate measurement of the inherent background, smoothing the profiles by Fourier analysis and synthesis, deconvolution and least-squares treatments. The method has been applied to data collected at 23 K, up to $2\theta_{Mo} = 100°$, from a spherical crystal of L-alanine. Model profiles are in excellent agreement with the experimental ones, and were used to evaluate truncation losses for several scan ranges. For the instrumental configuration of the diffractometer used in this investigation, scan-truncation losses are far larger than predicted by previous studies.

1. Introduction

It is well known that intensities of high-angle reflections are typically underestimated when measured on a scanning diffractometer, owing to the finite range of the scan. The intensity profiles of the reflections are broadened by $\alpha_1 - \alpha_2$ splitting and dispersion and by other effects related to the diffractometer and to the quality of the crystal; since the scan range must be limited to avoid overlap with neighboring reflections, some of the diffraction intensity will be lost. Since the amount of intensity loss - often called 'scan-truncation error' - depends on (among other things) the scattering angle, failure to correct for it will introduce systematic errors into the U_{ij}'s and the scale factor. For example, Eisenstein & Hirshfeld (1983), in deriving charge-deformation densities from low-temperature data extending to $2\theta = 140°$, found a 2θ-dependent background behavior that 'no plausible truncation model could account for', and note ruefully that 'the uncorrected truncation error and the consequent limitation on the deformation model combine to cast severe doubt on the absolute magnitudes of the refined atomic vibration parameters'.

In the case of powder diffraction data, the problem of truncation has long been recognized, and several procedures for its treatment have been suggested (Young, Gerdes & Wilson, 1967; Langford, 1982; and references therein). For single-crystal diffractometry, a paper by Alexander & Smith (1962; hereinafter AS) is usually cited as the pioneering work for the analysis of errors in intensity measurements. These authors presented first-order correction curves for truncation effects, based on a theoretical profile obtained by the convolution of four relevant functions. The problem has been subsequently discussed by several authors (Ladell & Spielberg, 1966; Young, 1969: Kheiker, 1969; Einstein, 1974, among others), but in practice truncation corrections have usually been neglected, at least until the appearance of the empirical procedure suggested by Denne (1977*a*). Even when optimal experimental conditions for a successful set of measurements are discussed (*e.g.* Rees 1977; Coppens, 1978; Lehmann, 1980), the truncation problem may be ignored, perhaps on the assumption that the effect is negligible compared with other experimental errors. Yet Hirshfeld & Hope (1980) report that truncation effects may cause F_o's to be underestimated by as much as 40% for high-angle data.

The approximate equation given by Denne (1977*a*) is based on the assumption that in the intensity profile 'the effect of finite source size, finite crystal size and mosaic spread will tend to average out.' The approximation might be valid when the monochromation technique proposed by Denne (1977*a*, *b*) is employed, but in general it is inappropriate. Indeed, some of those who have applied Denne's procedure (Hope & Ottersen, 1978; Ottersen & Hope, 1979; Eisenstein, 1979; Hirshfeld & Hope, 1980; Ottersen, Almlöf & Hope, 1980; Ottersen, Almlöf & Carle, 1982) have noted that the correction may have been insufficient, and it has been suggested (Eisenstein,

* Contribution No. 7479 from the Arthur Amos Noyes Laboratory of Chemical Physics.

† Permanent address: Dipartimento di Chimica Fisica ed Elettrochimica, Università di Milano, Via Golgi 19, Milano 20133, Italy.

0108-7673/87/050711-08$01.50

1979; Hirshfeld & Hope, 1980) that the correction be calculated as if the scanning of the profile had taken place over a narrower width than was actually used. Besides being somewhat arbitrary, this artificial modification emphasizes the inadequacy of the method. In Fig. 1, a profile (continuous line) calculated by Denne's procedure, and on which the truncation losses are evaluated by his method, is compared with the measured profile of reflection $0,\bar{2}0,7$ of L-alanine ($2\theta \simeq 92°$ for Mo $K\alpha$ radiation).

It is the purpose of the present paper to give further experimental evidence of the relevance of the problem, and to suggest an empirical approach which does not pretend to be free from limitations, but rather demands to be judged heuristically on the basis of its performance.

2. The method

The observed intensity profile results from the convolution of the intrinsic spectral distribution of the radiation with several instrumental effects - including crystal size and mosaicity and the intensity profile of the X-ray source. One might hope that the instrumental effects could be combined into a single function that would be independent of the scattering angle; if this were the case, this instrumental function could be deconvoluted by measuring an intensity profile at very low scattering angle (where the spectral distribution approximates a delta function) and could then be reconvoluted to yield theoretical profiles at all other angles. Unfortunately, we have found it necessary to introduce a third, angle-dependent, function - which we call an 'aberration function' - in order to satisfactorily reproduce our experimental scan profiles at all angles. When these three functions are convoluted, we obtain a total profile from which the effects of truncation can be confidently estimated.

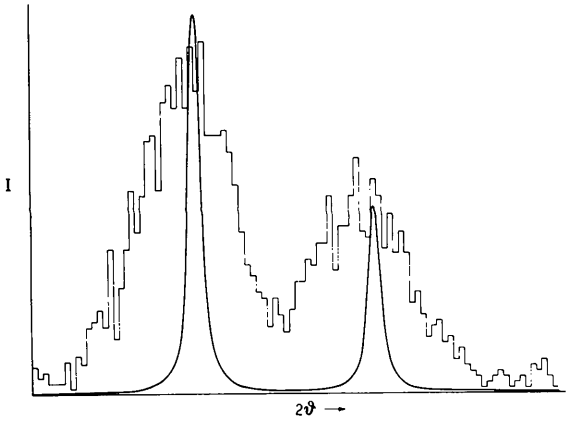

Fig. 1. Comparison between the experimental step-scan profile for reflection $0,\bar{2}0,7$ of L-alanine at 23 K ($2\theta_{Mo} \simeq 92°$) and the bimodal Cauchy function adopted by Denne (1977*a*) for the calculation of the truncation losses at the same 2θ value.

Using notation similar to that adopted by AS, we define three functions: I_b, the basic or intrinsic profile which includes the angle-independent components such as crystal size and mosaicity; I_λ, the spectral dispersion; and I_a, the angle-dependent aberration function, which presumably includes such instrumental effects as beam divergence, asymmetry and the like. The convolution of the first two functions yields the *idealized* synthetic profile

$$I(\beta)_{b\lambda} = \int I(\alpha)_b I(\alpha - \beta)_\lambda \, d\alpha \qquad (1)$$

where the variables α and β are angular displacements as in AS. The final synthetic profile is then

$$I(\beta)_{b\lambda a} = \int I(\alpha)_{b\lambda} I(\alpha - \beta)_a \, d\alpha \qquad (2)$$

and the total background-free integrated intensity will be

$$I_i = \int I(\beta)_{b\lambda a} \, d\beta. \qquad (3)$$

Besides the addition of the function I_a, our method for the reconstruction of an intensity profile differs from that of AS in that only one function, I_λ, is here calculated on the basis of theoretical components, while the other two are obtained from experimental measurements.

An essential point of the present approach is the fact that at very low values of 2θ the spectral dispersion function I_λ does not differ significantly (with respect to I_b, and in terms of β units) from a delta function. Therefore, we assume that I_b can be represented by the low-angle experimental profile itself. To a first approximation, the description of the spectral dispersion can be given by the proper combination of two Cauchy-like functions (Hoyt, 1932; Ekstein & Siegel, 1949). For the $K\alpha$ doublet, rather than adopting an analytical representation including asymmetry parameters (Ladell, Parrish & Taylor, 1959; Ladell, Zagofsky & Pearlman, 1975), or the modulated Lorentzian function proposed by Mignot & Rondot (1976), we maintain for each of the $K\alpha$ lines the simple approximate equation given by AS:

$$I(\beta)_\lambda = I_{max}/[1 + (2\beta/W_\lambda)^2] \qquad (4)$$

where the full width at half-maximum intensity is given by

$$W_\lambda = (\Delta\lambda/\lambda) \tan\theta \qquad (5)$$

and $\Delta\lambda$ values are taken from Compton & Allison (1935).

The remaining aberration function I_a is obtained by the deconvoluting process proposed by Stokes (1948). In Fourier analysis, the intensity profiles are treated as periodic functions known, in numerical form, at N points. If the Fourier components of the transform H of the experimental profile are indicated by $H(t)$ and those of the transform G of the idealized synthetic profile by $G(t)$, then the transform F of the

Table 1. *Details of data collection for a single crystal of* L-*alanine at* 23 *K*

	Number of reflections	Scan range* (°)		Scan rate (° min^{-1})	t_B/t_S†
Set 1	104		$3{\cdot}5+S$	0·5	1·0
Set 2	104	$2\theta<35°$	$2{\cdot}6+S$	0·5	1·0
		$35\le 2\theta<65°$	$2{\cdot}0+S$	0·5	1·0
		$65\le 2\theta<100°$	$1{\cdot}4+S$	0·5	1·0
Set 3	2535 (hkl)	As for set 1		Variable 2·0 to 4·0	0·7
Set 4	5070 ($hkl+h\bar{k}\bar{l}$)	As for set 2		As for set 3	1·0

* S is the $\alpha_1-\alpha_2$ separation.

† t_B = time for background measurements, at both ends of the scan range, each for a time equal to $\frac{1}{2}t_B$; t_S = scan time.

aberration function I_a has coefficients given by

$$F(t)=H(t)/aG(t). \tag{6}$$

In practice the proportionality factor $1/a$ can be omitted, and the real and imaginary parts of each $F(t)$ are

$$\begin{aligned} F_r &= (H_rG_r+H_iG_i)/(G_r^2+G_i^2) \\ F_i &= (H_iG_r-H_rG_i)/(G_r^2+G_i^2). \end{aligned} \tag{7}$$

Preliminary investigations showed that the fitting of the aberration-free function $I_{b\lambda}$ to the experimental profile at high angles was satisfactory in the peak region (say, down to 1/10 of the maximum value of the peak), but very poor in the tails, where the calculated values were much lower than the measured ones. We also noted severe asymmetries in the tails, the residuals at the high-angle ends of the scans being larger than those at the low-angle ends; thus, the imaginary (antisymmetric) terms F_i in the transform of the aberration function were expected to be important.

We are aware of the limitations of Fourier methods in investigating intensity profiles (Young, Gerdes & Wilson, 1967), and we emphasize that our interest here is not in the derivation of physical information from profile analysis. Rather, our approach is aimed at obtaining a satisfactory model for an experimental profile, so that a reliable estimate of the truncation error can be made.

3. Experimental

The sample used in our measurements was a crystal of L-alanine, ground to a sphere of radius 0·18 mm and mounted on the tip of a Pyrex glass fiber. Details of the data collection are given in Table 1. At the temperature of measurements [23(1) K], crystallographic data for L-alanine are: $a=5{\cdot}928\,(1)$, $b=12{\cdot}260\,(2)$, $c=5{\cdot}794\,(1)$ Å; orthorhombic, space group $P2_12_12_1$; $Z=4$. Data were collected in the θ–2θ scan mode on a computer-controlled four-circle diffractometer modified for low temperatures (Samson, Goldish & Dick, 1980). In this apparatus the sample crystal is enclosed in an evacuated ($P<2{\cdot}7\times10^{-3}$ Pa) spherical chamber about 150 mm in diameter. The detector, with a circular receiving aperture 2·0 mm in diameter, was placed very close to the outer surface of the chamber to minimize air-scattering effects. The diffractometer was equipped with an Mo-target General Electric X-ray tube, type CA-8-S, operating at 45 kV and 15 mA. The radiation was monochromatized by a graphite crystal, set at the configuration corresponding to $\varepsilon=0°$ (Arndt & Willis, 1966). Backgrounds were always collected with the counter stationary.

Table 2. *Average increase* (%) *of apparent net intensity upon enlarging the scan range for the* 104 *reflections of sets* 1 *and* 2

2θ interval (°)	Number of reflections	ΔI*
10–20	5	0·36
20–35	10	3·73
35–65	18	6·37
65–100	71	7·10

* $\Delta I=\langle(I_1-I_2)/I_2\rangle\times100$.

Data sets 1 and 2 (Table 1) were based on a selection of relatively strong reflections predicted from the known crystal structure (Simpson & Marsh, 1966); sets 3 and 4 include all reflections within the specified ranges. The 2θ scan range of $(3{\cdot}5+S)°$ used for data sets 1 and 3 was chosen as the largest feasible range that avoids overlap with neighboring reflections. For sets 2 and 4, the variation of scan range with 2θ is opposite to that usually used, the reason being that as 2θ increases, the intensities and their relative precisions decrease, so that the truncation effects could be accurately evaluated only if the effects were relatively large and, hence, the scan ranges relatively small.

Evaluation of the preliminary data represented by sets 1 and 2 led to two conclusions: (i) the corrections for truncation losses appeared to be far larger than predicted by AS; (ii) for reflections with 2θ greater than 65°, truncation losses are large even for the expanded scan range of $(3{\cdot}5+S)°$. In Table 2 are given the percentage increases in *apparent* net intensities in going from set 2 to set 1; the leveling off of this increase (ΔI) at large 2θ values is a manifestation of the large truncation losses even in set 1. These conclusions were confirmed by analysis of several hundred of the stronger reflections from sets 3 and 4.

4. Background correction

In order to assess truncation losses, we first need an accurate measurement of inherent background in the region of the reflection under consideration. If we assume that thermal diffuse scattering is negligible at

the temperature of our measurements and that for this spherical crystal the inherent background varies only with 2θ, we can evaluate this background by making measurements either at points far distant from any reciprocal-lattice point or by simply averaging the background counts made on both sides of the weak reflections measured with the expanded scan range (sets 1 and 3). We have used both methods and found that they indeed agree very well (see Fig. 2). However, both methods indicate a large background anomaly at $2\theta \sim 10°$ and a smaller one at $2\theta \sim 30°$. Suspecting that these anomalies were due to the glass fiber and glue supporting the crystal, we repeated the measurements with the crystal removed; this curve indeed contained the same anomalies (Fig. 2). We further note that, when we used the same fore-and-aft backgrounds from the reduced scan-range measurements (sets 2 and 4), the averaged background curve was higher by about 0·3–0·4 counts s^{-1} at all angles, indicating noticeable truncation losses for even the very weak reflections.

We note in passing that the high-2θ ('aft') background measurements are systematically larger than the low-2θ ('fore') measurements, for both the reduced and (less dramatically) for the expanded scan ranges. This phenomenon, particularly noticeable on our diffractometer, is an instrumental effect that we believe is related to the monochromator arrangement. Indeed, when intensity profiles from our alanine crystal, as well as from other crystals, were recorded on another diffractometer that had the graphite crystal in the same configuration ($\varepsilon = 0°$), a similar marked asymmetry in the tail regions was observed. On the other hand, a much different pattern, with very reduced or no asymmetry, was shown by profiles derived from some of those same crystals when mounted on a diffractometer with the graphite monochromator in the configuration corresponding to $\varepsilon = 90°$.

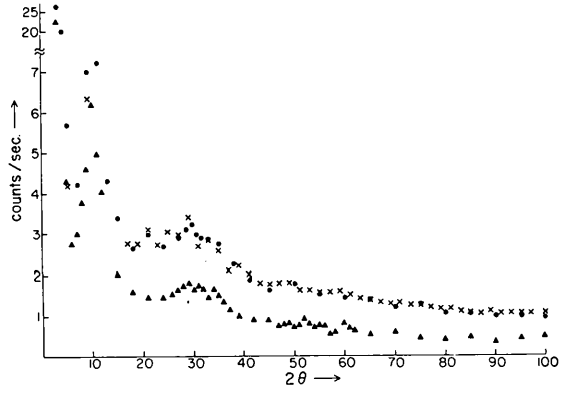

Fig. 2. Background distribution for L-alanine at 23 K. Upper points: average distribution (×) of the background for the 783 reflections of set 3 with $I < 6\sigma(I)_{c.s.}$ superimposed on measurements (●), each for 100 s, at points far distant from reciprocal-lattice points (stationary crystal, arbitrary orientation, $\varphi = 90°$, $\chi = 0°$). Lower points (▲): contribution to the background due to the scattering of the air and specimen support (crystal removed).

We made a rapid non-systematic search for φ or χ dependence of the inherent background and found no trend. Accordingly, in our subsequent truncation studies we assigned backgrounds from an interpolation table constructed from the curve in Fig. 2. We note the generally low level of the background - about 1 count s^{-1} at high angles - and the absence of extraneous effects (other than those due to the glass fiber), strong testimonials to the performance of the low-temperature diffractometer (Samson, Goldish & Dick, 1980).

5. Application of the method

The basic profile I_b, expressed as a set of points at intervals of 0·01°, was obtained by the treatment of three low-angle ($2\theta < 10°$) reflections. The process included removal of the background, normalization to a common value for the total area under the peak, and smoothing (by graphical interpolation).

Of the 2535 reflections from set 3, a selection of 93 relatively strong intensities was made, such as to include at least four measurements within each of the ten 10° intervals of 2θ. Each of the 93 profiles underwent the following treatment: (i) removal of the background and normalization; (ii) substitution of the first and last of the 96 profile steps by the more reliable values derived from the lengthier measurements of background; (iii) smoothing to eliminate most of the local statistical variations. This last step was performed by numerical Fourier methods: after evaluation of the transform of the profile, the high-frequency components judged to be of little significance were disregarded, and the remaining terms were used to generate by Fourier synthesis a smoothed profile (I_{exp}) at 0·01° steps. Reasons for this procedure will be given below.

The corresponding 93 idealized (aberration-free) synthetic profiles $I_{b\lambda}$ were obtained by folding the basic profile with the appropriate spectral distribution functions I_λ [(4)], computed within the limits $0{\cdot}68926 < \lambda < 0{\cdot}73354$ Å. This range of wavelength values, equivalent to $(\lambda\alpha_1 - 0{\cdot}02) - (\lambda\alpha_2 + 0{\cdot}02)$ Å for Mo $K\alpha$ radiation, covers 99·54% of the bimodal Cauchy-shaped distribution. The resulting $I_{b\lambda}$ profiles, again calculated at 0·01° intervals, were normalized and the portions corresponding to the experimental scan range were kept for subsequent use in the unfolding process. The function $I_{b\lambda}$ for a high-angle reflection (0,20,7, $2\theta = 92{\cdot}19°$) is compared with the background-free non-smoothed experimental profile in Fig. 3(*a*). It is evident, as already mentioned in § 2, that the peaks themselves are well reproduced ($K\alpha_1$ perhaps better than $K\alpha_2$), while at the tails the experimental measurements systematically exceed the

calculated values. The same behavior occurs for relatively low-angle reflections (Fig. 3*b*), but here the peaks too are slightly but significantly different, the calculated being somewhat narrower and higher. It may therefore be anticipated that the aberration function should be 2θ dependent.

To find the Fourier components of the aberration function I_a that broadens $I_{b\lambda}$, the deconvolution of I_{exp} and $I_{b\lambda}$ was performed for each of the 93 profiles, according to (6) and (7). As expected, inspection of the low-frequency, more significant, components showed a slowly varying but well defined 2θ dependence. Instead of attempting to parameterize this dependence by a set of analytical functions of 2θ we chose, for simplicity, to evaluate averages of the I_a function within discrete 2θ ranges. Each of the real and imaginary parts of the Fourier components $F(t)$ was assigned an approximate variance σ_t^2 proportional to $[G^2(t)+H^2(t)]/G^4(t)$ (Stokes, 1948), where $G(t)$ and $H(t)$ are the Fourier components of $I_{b\lambda}$ and I_{exp} respectively. A weighted average - including all reflections measured within a given interval of the 2θ scan range - yielded the mean transform F' of I_a for that interval. In the averaging process, each profile was given a weight equal to the square root of its net scan intensity P; hence, each term had a weight $w_t = P^{1/2}/\sigma_t^2$.

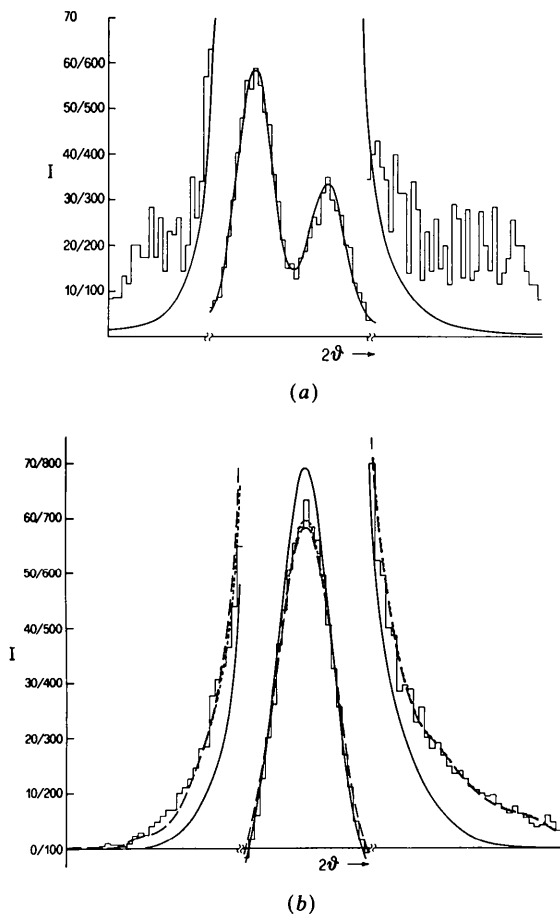

Fig. 3. (*a*) The idealized aberration-free synthetic profile $I_{b\lambda}$ (continuous line) for a high-angle reflection, superimposed on its background-free non-smoothed experimental profile. (*b*) For reflection 260 ($2\theta_{Mo} \simeq 24°$) of L-alanine, the experimental profile (histogram) is compared with its aberration-free synthetic profile (continuous line) $I_{b\lambda}$, and with two final synthetic profiles $I_{b\lambda a}$. One of the latter (- - - -) was obtained by convoluting $I_{b\lambda}$ with the aberration function derived from the same reflection 260, the other (— — —) using the aberration function derived from reflection 033 ($2\theta_{Mo} \simeq 23°$). These latter two curves are nearly indistinguishable.

In accordance with the multiplicative properties of transforms, which are also valid for the individual coefficients, the components of the transforms H' of the distorted (by the aberration function) synthetic profiles were computed as $H'(t) = F'(t)G(t)$; a Fourier synthesis then gave the final model profile for each 2θ range. From these model profiles the losses due to truncation can be evaluated for any desired scan range.

In the performance of the procedure so far described, several points had to be treated with particular care. Among others, the following are noteworthy:

(1) For a proper treatment (comparison and averaging) of the transform components of different profiles, the discrete intervals at which the 'periodic functions' are known must have the same values. On the other hand, owing to the variable-scan techniques employed in data collection, all profiles are measured at 96 equally-spaced points, so that the range value of each step varies with the 2θ value of the reflection. One way to cope with this problem is to vary the arbitrary periodicity a of the profile functions, so that the interval between two steps could be given as the same fraction of a for all reflections. We preferred to perform a cyclic Fourier process (analysis and synthesis, the latter at a fixed interval of 0·01°), because of the contemporaneous elimination of insignificant high-frequency terms (the smoothing process mentioned above).

(2) The numerical values of the real and imaginary parts of the Fourier components strongly depend on the choice of origin for the period a. This means that the unfolding of I_{exp} and $I_{b\lambda}$ must be preceded by an accurate and equivalent definition of a common center of two profiles to be deconvoluted. Obviously enough, such a precaution would not be required (*i.e.* the choice of origin could be totally arbitrary for each individual profile) if a single individual aberration function I_a were to be evaluated. It is the averaging of the aberration functions that requires all transforms to be computed with a procedure as similar as possible.

(3) All profiles above a certain 2θ value are naturally asymmetric (because of $K\alpha_1 - K\alpha_2$ splitting); hence, the imaginary terms of the Fourier

components play a fundamental role, and the cut-off value of $H(t)$ for the elimination of spurious details cannot be based on the real terms alone, as one might infer from Stokes's example. Several numerical tests, made both on experimental profiles and on modified Gaussian-type functions, showed that a Fourier synthesis based on the first t terms for which $[H_r^2(t)+H_i^2(t)]^{1/2} \geq 0{\cdot}5\%$ of $H_r(0)$ gave a more than satisfactory reconstruction of the functions.

We note two limitations in our procedure:

(i) the Fourier method for smoothing the experimental profiles, while effective in removing local statistical variations, cannot avoid an oscillating behavior in the region of the tails, and these tails are critical in assessing truncation effects;

(ii) as indicated by Stokes (1948), an optimal condition for the deconvolution process is that the functions to be unfolded be very different in shape, *i.e.* $I_{b\lambda}$ be much narrower than $I_{\exp}$. This is not true in the present case.

We have made an extensive set of preliminary tests to verify how severe these limitations are, and found that they do not hamper the attainment of the main result - the description of I_a (and hence of truncation losses) in its essential features. For instance, we found that for a given reflection the first important terms, up to $t=15$, of the transform of the corresponding I_a were essentially the same irrespective of the treatment of the details of the experimental profiles. In other words, no significant differences were detectable in those 15 terms when the experimental profile was: (i) smoothed according to the procedure described above; (ii) smoothed by analytical and graphical methods such as to have a monotonically decreasing function; (iii) treated without any smoothing procedure, taking the experimental values corrected for background only. Another interesting result came from an early investigation on 12 reflections collected in the range $20<2\theta<26°$. From each of them the transform of I_a was computed, and the resulting final synthetic profile was compared with the experimental values. The quantity

$$R=\sum_1^{96}|\Delta h_i|\Big/\sum_1^{96} h_i,$$

where h_i is the measured intensity at each of the 96 profile steps and Δh_i the corresponding difference between experiment and model, never exceeded 0·04. (Subsequently the R index was evaluated for all 93 reflections; only for the weakest intensities was its value significantly higher, up to 0·10.) Even more interestingly, similar values (0·04–0·06) were obtained when the final synthetic profile of a given reflection was computed by convolution of its $I_{b\lambda}$ and an aberration function derived from *different* reflections of similar 2θ value. A small portion of these results is shown in Fig. 3(*b*), where the experimental profile of reflection 260 is compared with its aberration-free idealized synthetic profile $I_{b\lambda}$, and with final synthetic profiles for both the 260 and 033 reflections; the improvement due to the inclusion of I_a in the treatment and the practical coincidence of I_a for both reflections are both evident. This series of results suggested the calculation of average aberration functions for a given 2θ range and, in our opinion, proves the reliability of the method.

It is true, however, that undesired oscillations appear in the outermost regions of the final model profile, as seen in Fig. 3(*b*); this is the region in which a monotonic behavior is required for a proper evaluation of the truncation errors. Since the tailing off of the profile is mainly due to the spectral dispersion, a least-squares fit to a Cauchy function was considered the appropriate procedure to smooth these tails and yield a uniformly decreasing shape. Only points in the proximity of the scan-range extrema were included in this least-squares treatment. The results were checked by comparing the values of steps 1 and 96 of the experimental profile (corrected for background as described above) with the calculated quantities. In all cases the differences were less than the e.s.d. based on counting statistics.

6. Results and discussion

In Table 3 are given the truncation losses for various scan ranges in 2θ values, calculated from the intensity functions we have derived. We separate these losses into two parts (see Fig. 4): the part B that is within the scan range and is due to overestimation of the background, and the two portions C due to the tailing of the profile beyond the scan limits. Proper evaluation of C requires an extrapolation of the sort we have done here. Part B can also be estimated merely by subtracting the inherent background (as measured for the weak reflections or at non-lattice points; see Fig. 2) from the experimental background; we have evaluated it this latter way as well, using the measured backgrounds of the 1050 strongest reflections of set 3 (Table 1), and found essentially exact agreement with the values that are obtained from Table 3. For normal scan ranges of 2° or so, portion C is appreciably smaller than B but by no means negligible. In Fig. 4 are plotted portions B and C for the two extreme scan ranges we investigated ($1{\cdot}4+S$ and $3{\cdot}5+S$, where S is the $\alpha_1-\alpha_2$ splitting).

Two features of Table 3 and Fig. 4 are notable: (1) the truncation losses are far larger than predicted by AS (1962) or by Denne (1977*a*); for instance, whereas Denne predicted a loss of about 6% for a scan range of $(2+S)°$ at $2\theta=90°$ (Mo radiation) we find a loss of about 15%. (2) All our curves show a dip at about $2\theta=74°$. While we have no understanding as to the source of this dip, we believe it to be real; it is a

Table 3. *Truncation losses, obtained from the calculated intensity profiles, for four scan ranges*

The losses are expressed as percentages of the uncorrected measured intensity. S is the $K\alpha_1 - K\alpha_2$ splitting for Mo radiation.

	Total loss $[100(B+C)/A]$ Scan range (°2θ)				Tails only $(100C/A)$ Scan range (°2θ)			
2θ (°)	1·4+S	2·0+S	2·6+S	3·5+S	1·4+S	2·0+S	2·6+S	3·5+S
5	5·4	1·9	1·2	0·2	1·2	0·3	0·2	0·0
15	8·3	3·6	2·0	0·2	2·1	0·7	$0·2_5$	0·0
25	13·7	7·2	4·2	1·2	4·4	1·8	0·7	0·1
35	17·6	$11·1_5$	$7·1_5$	2·9	6·6	3·2	1·3	0·3
45	18·1	13·1	9·8	5·0	7·4	4·2	2·0	0·7
55	18·0	13·7	11·0	7·0	7·7	4·7	$2·4_5$	$1·0_5$
65	15·8	11·9	10·6	8·2	6·7	4·1	$2·2_5$	1·5
75	16·5	12·6	10·7	7·5	6·6	4·3	$2·3_5$	1·0
85	17·5	13·6	11·5	8·8	7·0	4·5	$2·7_5$	1·6
95	(27)	$16·8_5$	14·6	$12·1_5$	(8·2)	5·7	3·9	2·2

manifestation of the 2θ dependence of the aberration function I_a.

We emphasize that the results we report here are applicable only to our particular experiment. As noted previously, preliminary experiments strongly suggest that the same crystal, when mounted on a different diffractometer, can give rise to much different scan profiles and hence different 'aberration' functions. We cannot anticipate whether truncation effects would also be different. Thus, the numbers in Table 3 should not be used in other laboratories; rather, they should be accepted only as indicators of the importance of truncation under some particular experimental conditions. We urge that, in experiments where accurate intensity measurements are needed (such as studies on thermal motion or on electron density distributions), investigators make truncation corrections of the type outlined here, but based on the same crystal and instrumental arrangement as used in recording the intensities.

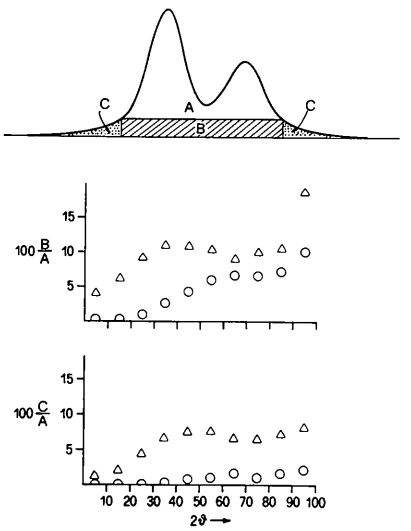

Fig. 4. Plots of the calculated truncation losses at different $2\theta_{Mo}$ values for two scan ranges, $(1·4+S)°$ (△) and $(3·5+S)°$ (○), where S is the $K\alpha_1 - K\alpha_2$ separation for Mo radiation.

Note added during publication. Since originally submitting this manuscript, we have carried out a similar truncation analysis on a second crystal, with analogous but not identical results.

The second crystal was of citrinin [space group $P2_12_12_1$, $a = 13·242\,(3)$, $b = 7·237\,(1)$, $c = 12·136\,(3)$ Å at 19·5 K; see Destro & Marsh (1984)]. It was ground to a sphere of radius approximately 0·19 mm. Two sets of data were collected at 19·5 K, set 1 comprising 9091 reflections (including checks) up to $2\theta = 110°$ and set 2 comprising 280 profiles chosen from the strongest reflections of set 1. For set 1 the scan rate was variable from 2·0 to 6·0° min^{-1}, the scan range was $(2·2+S)°$ and $t(b)/t(S)$ was 0·5; for set 2 the scan rate varied from 0·5 to 2·0° min^{-1}, the range was $(3·0+S)°$ and $t(b)/t(S)$ was 1·0. There were three instrumental differences with respect to the alanine data: (*a*) the X-ray tube was from Siefert rather than General Electric; (*b*) the operating current was 20 rather than 15 mA; (*c*) the monochromator was in the perpendicular geometry ($\varepsilon = 90°$).

The background distribution, derived from 5588 reflections from set 1 with $I < 6\sigma(I)$ plus 224 measurements between Bragg points, showed the same features at $2\theta = 10$ and 30° as observed for alanine; the backgrounds were uniformly higher, by about 1 count s^{-1}, than those in Fig. 2, presumably because of the higher tube current. Unlike the alanine data, there was very little asymmetry in the profile tails of the stronger reflections (see § 4).

Processing of the 280 profiles of set 2 followed essentially the same procedure as for alanine; the reflection chosen for the basic profile was 101 ($2\theta = 4·54°$). The least-squares treatment of the Cauchy function used to approximate the tails included a somewhat larger 2θ range within the profiles, chosen after a more careful inspection of the tails.

For these citrinin data, the total truncation losses reached a maximum of 17·8% for the scan range $(2·2+S)°$ and a maximum of 13·9% for $(3·0+S)°$,

both maxima occurring at $2\theta = 85°$. These numbers are appreciably larger than found for alanine (Table 3; Fig. 4); most of the increase comes from the tails, and may be due to the different method of treating the least-squares fit to the Cauchy function. The 2θ dependence of the truncation losses indicated by the citrinin data is similar, but by no means identical, to that shown in Fig. 4, emphasizing once more that these corrections must be considered entirely empirical.

This investigation was supported in part by Public Health Service Research Grant no. 16966 from the National Institutes of Health.

References

ALEXANDER, K. E. & SMITH, G. S. (1962). *Acta Cryst.* **15**, 983-1004.
ARNDT, U. W. & WILLIS, B. T. M. (1966). *Single Crystal Diffractometry*, p. 287. Cambridge Univ. Press.
COMPTON, A. H. & ALLISON, K. S. (1935). *X-rays in Theory and Experiment.* New York: Van Nostrand.
COPPENS, P. (1978). *Neutron Diffraction*, edited by H. DACHS, pp. 79-92. Berlin, Heidelberg, New York: Springer-Verlag.
DENNE, W. A. (1977*a*). *Acta Cryst.* A**33**, 438-440.
DENNE, W. A. (1977*b*). *Acta Cryst.* A**33**, 987-992.
DESTRO, R. & MARSH, R. E. (1984). *J. Am. Chem. Soc.* **106**, 7269-7271.
EINSTEIN, J. R. (1974). *J. Appl. Cryst.* **7**, 331-344.
EISENSTEIN, M. (1979). *Acta Cryst.* B**35**, 2614-2625.
EISENSTEIN, M. & HIRSHFELD, F. L. (1983). *Acta Cryst.* B**39**, 61-75.
EKSTEIN, H. & SIEGEL, S. (1949). *Acta Cryst.* **2**, 99-104.
HIRSHFELD, F. L. & HOPE, H. (1980). *Acta Cryst.* B**36**, 406-415.
HOPE, H. & OTTERSEN, T. (1978). *Acta Cryst.* B**34**, 3623-3626.
HOYT, A. (1932). *Phys. Rev.* **40**, 477-483.
KHEIKER, D. M. (1969). *Acta Cryst.* A**25**, 82-88.
LADELL, J., PARRISH, W. & TAYLOR, J. (1959). *Acta Cryst.* **12**, 561-567.
LADELL, J. & SPIELBERG, N. (1966) *Acta Cryst.* **21**, 103-122.
LADELL, J., ZAGOFSKY, A. & PEARLMAN, S. (1975). *J. Appl. Cryst.* **8**, 499-506.
LANGFORD, J. I. (1982). *J. Appl. Cryst.* **15**, 315-322.
LEHMANN, M. S. (1980). *Electron and Magnetization Densities in Molecules and Crystals*, pp. 287-314. New York: Plenum Press.
MIGNOT, J. & RONDOT D. (1976). *J. Appl. Cryst.* **9**, 460-465.
OTTERSEN, T., ALMLÖF, J. & CARLE, J. (1982). *Acta Chem. Scand. Ser. A*, **36**, 63-68.
OTTERSEN, T., ALMLÖF, J. & HOPE, H. (1980). *Acta Cryst.* B**36**, 1147-1154.
OTTERSEN, T. & HOPE, H. (1979). *Acta Cryst.* B**35**, 373-378.
REES, B. (1977). *Isr. J. Chem.* **16**, 154-159.
SAMSON, S., GOLDISH, E. & DICK, C. J. (1980). *J. Appl. Cryst.* **13**, 425-432.
SIMPSON, H. J. JR & MARSH, R. E. (1966). *Acta Cryst.* **20**, 550-555.
STOKES, A. R. (1948). *Proc. Phys. Soc. London Sect. A*, **61**, 382-391.
YOUNG, R. A. (1969). *Acta Cryst.* A**25**, 55-66.
YOUNG, R. A., GERDES, R. J. & WILSON, A. J. C. (1967). *Acta Cryst.* **22**, 155-162.

Acta Cryst. (1987). A**43**, 718-727

Equations for Diffuse Scattering from Disordered Molecular Crystals

BY RITA KHANNA* AND T. R. WELBERRY

Research School of Chemistry, Australian National University, PO Box 4, Canberra City, ACT 2601, Australia

(*Received* 26 *February* 1987; *accepted* 11 *May* 1987)

Abstract

General equations are presented for diffuse scattering due to static substitutional and orientational disorder in molecular crystals. Scattering due to displacements, both static and dynamic, and molecular librations is treated separately. Examples of a pair of isostructural isomers of dibromodiethyldimethylbenzene, which show very different disorder diffuse scattering, are given. Procedures for data analysis and separation of various diffuse scattering components are discussed.

Introduction

Since the early experiments of Wilchinsky (1944), Cowley (1950) and Warren, Averbach & Roberts (1951), most quantitative studies of diffuse X-ray and neutron scattering from disordered materials have been carried out on metallic alloys. The techniques for data and error analysis have become reasonably well established; see Borie & Sparks (1971), Gragg, Hayakawa & Cohen (1983), Hayakawa & Cohen

* Permanent address: Materials Science Laboratory, Indira Gandhi Centre for Atomic Research, Kalpakkam, 603102 India.

0108-7673/87/050718-10$01.50